

# Effect of Pr scattering on the penetration depth $\lambda_{ab}$ in $\text{Bi}_2\text{Sr}_2\text{Ca}_{1-x}\text{Pr}_x\text{Cu}_2\text{O}_{8+\delta}$ single crystals

X.-G. Li

*Department of Physics, National Tsing Hua University, Hsinchu 300, Taiwan  
and Structure Research Laboratory, University of Science and Technology of China, Anhui 230026, China*

X. F. Sun

*Structure Research Laboratory, University of Science and Technology of China, Anhui 230026, China*

Y. H. Toh, Y. Y. Hsu, and H. C. Ku

*Department of Physics, National Tsing Hua University, Hsinchu 300, Taiwan*

(Received 22 October 1997)

Four superconducting single crystals near the optimum-doped region ( $x=0, 0.11, 0.17,$  and  $0.28$ ) for the  $\text{Bi}_2\text{Sr}_2\text{Ca}_{1-x}\text{Pr}_x\text{Cu}_2\text{O}_{8+\delta}$  system were chosen for detailed structural and magnetic measurements, in order to study the effect of Pr scattering on the temperature dependence of the  $ab$ -plane penetration depth  $\lambda_{ab}$ . The penetration depth for these incommensurate modulated single crystals follows a  $T^2$  behavior at low temperature, and then crossover to a linear  $T$  dependence at the characteristic temperature  $T^*$ . Variation of linear  $T$  region and  $T^*$  with increasing Pr content indicates that Pr acts as a strong scattering center that modifies the local density of states of the system. The present result is consistent with the prediction for disorder-affected  $d$ -wave superconductors. [S0163-1829(98)01326-5]

## I. INTRODUCTION

It is extremely important to understand the symmetry of high- $T_c$  superconductors. Studies on the electromagnetic penetration depth  $\lambda$  at a temperature well below  $T_c$  are beginning to yield a consistent picture on the pairing state of high- $T_c$  systems.<sup>1-11</sup> For example, recent penetration depth measurements on high-quality single crystals of  $\text{YBa}_2\text{Cu}_3\text{O}_{7-y}$  and  $\text{Bi}_2\text{Sr}_2\text{CaCu}_2\text{O}_{8+\delta}$  gave strong support to  $d$ -wave symmetry.<sup>2</sup> In  $\text{YBa}_2\text{Cu}_3\text{O}_{7-y}$ , the temperature dependence of the penetration depth was found to be linear in a wide temperature range,<sup>1,2</sup> while some other experiments often show a  $T^2$  dependence<sup>3-9</sup> instead of the linear  $T$  characteristic expected for a clean  $d$ -wave superconductor. The discrepancy can be interpreted qualitatively as due to impurity or disorder scattering for a dirty  $d$ -wave superconductor. Particularly, Hirschfeld and Goldenfeld<sup>10</sup> predicted that there exists a crossover temperature  $T^*$  at which the dependence changes from the  $T$  to  $T^2$  law due to impurity defect and disorder scattering. Recently, the temperature dependence of the penetration depth on  $T_c$  in  $\text{Bi}_2\text{Sr}_2\text{CaCu}_2\text{O}_{8+\delta}$  was reported.<sup>11</sup> Samples with a maximum  $T_c$  show a linear behavior, while those with significantly reduced  $T_c$  follow a quadratic law. Since only the oxygen content  $\delta$  is changed, it is not clear why the penetration depth follows a linear law in some samples, but not in all samples.

In order to study the effect of disorder substitution on the temperature dependence of the penetration depth, the  $\text{Bi}_2\text{Sr}_2\text{Ca}_{1-x}\text{Pr}_x\text{Cu}_2\text{O}_{8+\delta}$  system is a good candidate due to the similar ionic radius of  $\text{Pr}^{3+}$  of 1.126 Å compared with  $\text{Ca}^{2+}$  of 1.12 Å. There have been many previous studies on the Pr-substituted systems.<sup>12-14</sup> However, previous studies are all on polycrystalline samples, which present very strong impurity scattering. In this paper, impurity-free clean single-

crystal penetration depth data on the Pr-substituted  $\text{Bi}_2\text{Sr}_2\text{Ca}_{1-x}\text{Pr}_x\text{Cu}_2\text{O}_{8+\delta}$  system are reported.

## II. EXPERIMENTS

Single crystals of the  $\text{Bi}_2\text{Sr}_2\text{Ca}_{1-x}\text{Pr}_x\text{Cu}_2\text{O}_{8+\delta}$  system were grown using the standard self-flux method. High-purity  $\text{Bi}_2\text{O}_3$ ,  $\text{SrCO}_3$ ,  $\text{CaCO}_3$ ,  $\text{Pr}_6\text{O}_{11}$ , and  $\text{CuO}$  powders with the off-stoichiometric ratio were mixed, ground, and calcined in air for 1 day. The reacted powders with excess  $\text{Bi}_2\text{O}_3$  included as a flux were then used for crystal growth. The details for crystal growth will be described elsewhere.<sup>15</sup> The actual composition of the as-grown single crystals was determined from an energy dispersive x-ray (EDX) analysis using a Leica Stereoscan 440 scanning electron microscopy. The average size of the single crystals was 4 mm×2 mm×0.04 mm. All single crystals were post-annealed at 360 °C in air for 3 days to ensure sample homogeneity.

Single-crystal x-ray data were obtained with a Rigaku Rotaflex 18-kW rotating anode x-ray diffractometer using graphite monochromatized  $\text{Cu } K\alpha$  radiation with a scanning rate of 0.5°–1° in  $2\theta$  per minute. For the  $a$ -axis and  $b$ -axis x-ray diffraction measured in the transmission fashion, a fiber sample attachment with a divergence slit of 1/6° was used. All x-ray diffraction data were collected through careful alignment of the  $a$ ,  $b$ , and  $c$  axes of the crystals. The anisotropic magnetic susceptibility  $\chi_{ab}(T)$  and magnetization  $M_{ab}(H)$  measurements were carried out with a  $\mu$ -metal-shielded Quantum Design MPMS<sub>2</sub> superconducting quantum interference device (SQUID) magnetometer down to 5 K in an applied magnetic field from 1 G to 10 kG.

## III. RESULTS AND DISCUSSION

Four superconducting single crystals near the optimum-doped region ( $x=0, 0.11, 0.17,$  and  $0.28$ ) for the

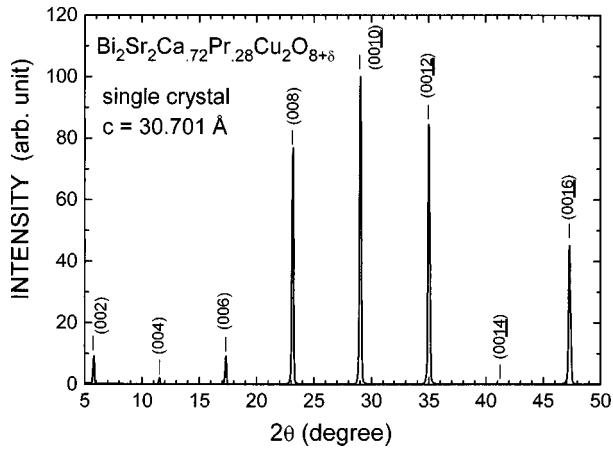


FIG. 1. X-ray diffraction pattern of orthorhombic (00*l*) lines for  $\text{Bi}_2\text{Sr}_2\text{Ca}_{0.72}\text{Pr}_{0.28}\text{Cu}_2\text{O}_{8+\delta}$  single crystal.

$\text{Bi}_2\text{Sr}_2\text{Ca}_{1-x}\text{Pr}_x\text{Cu}_2\text{O}_{8+\delta}$  system were chosen for detailed studies. Figure 1 shows a typical *c*-axis x-ray diffraction pattern for the single-crystal  $\text{Bi}_2\text{Sr}_2\text{Ca}_{0.72}\text{Pr}_{0.28}\text{Cu}_2\text{O}_{8+\delta}$ . No impurity lines were observed, and the Bi-2212-type (00*l*) diffraction lines give an orthorhombic *c* parameter of 30.701 Å. The *b*-axis diffraction pattern in Fig. 2 gives a *b* parameter of 5.439 Å and an incommensurate modulation along the *b* axis with period  $s = 4.56$ . No modulation was observed along the orthorhombic *a* axis ( $a = 5.435$  Å).

The orthorhombic unit-cell volume increases from 902.3 Å<sup>3</sup> for  $x = 0$  to 907.6 Å<sup>3</sup> for  $x = 0.28$  and 912.1–922.5 Å<sup>3</sup> for  $x = 1$ ,<sup>16</sup> due to extra incorporated oxygen and a slightly larger ionic radius of  $\text{Pr}^{3+}$  of 1.126 Å compared with  $\text{Ca}^{2+}$  of 1.12 Å. The incommensurate modulation period along *b* axis decreases from  $s = 4.76$  for  $x = 0$  to 4.56 for  $x = 0.28$  and 4.16 for  $x = 1$ , and the *c* parameter decreases monotonically from 30.849 Å for  $x = 0$  to 30.701 Å for  $x = 0.28$  and 30.267–30.363 Å for  $x = 1$ .<sup>16</sup> The decreasing *c* parameter is probably due to one or more of the following reasons: (i) With increasing Pr content, the incorporated oxygen with positive charge in the  $\text{Bi}_2\text{O}_3$  double layers increases and, consequently, causes the slab sequence SrO-BiO-BiO-SrO to

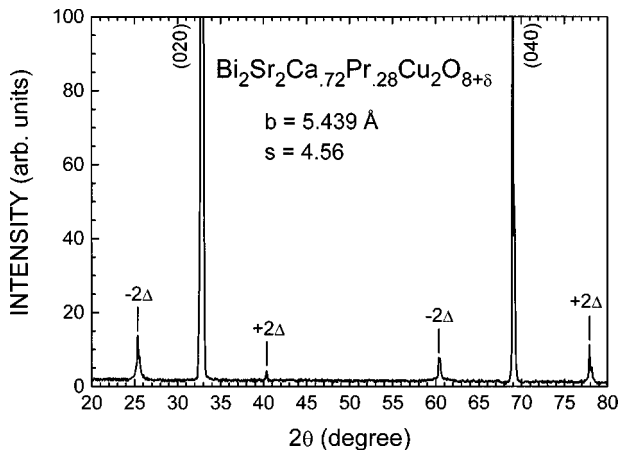


FIG. 2. X-ray diffraction pattern of orthorhombic (0*k*0) lines for a  $\text{Bi}_2\text{Sr}_2\text{Ca}_{0.72}\text{Pr}_{0.28}\text{Cu}_2\text{O}_{8+\delta}$  single crystal. Incommensurate modulation lines are denoted by  $\pm 2\Delta$ .

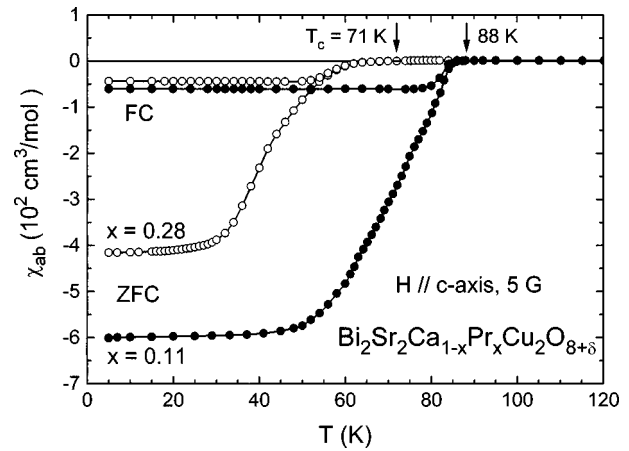


FIG. 3. Molar magnetic susceptibility  $\chi_{ab}(T)$  with low applied magnetic field parallel to the *c* axis of superconducting  $\text{Bi}_2\text{Sr}_2\text{Ca}_{1-x}\text{Pr}_x\text{Cu}_2\text{O}_{8+\delta}$  single crystals ( $x = 0.11, 0.28$ ) in field-cooled (FC) and zero-field-cooled (ZFC) modes.

shrink. (ii) With Pr doping, an additional band crosses the Fermi level, grabbing holes from the Cu-O  $d_{\sigma-p}$  band. The attractive interaction should result in the decrease of the separation between two  $\text{CuO}_2$  layers. (iii) With predominant  $\text{Pr}^{3+}$  character, there may still exist some  $\text{Pr}^{4+}$  character<sup>16</sup> with a smaller ionic size compared with  $\text{Ca}^{2+}$ .

The *ab*-plane magnetic susceptibility  $\chi_{ab}(T)$  with a 5-G low field parallel to the *c* axis of  $\text{Bi}_2\text{Sr}_2\text{Ca}_{1-x}\text{Pr}_x\text{Cu}_2\text{O}_{8+\delta}$  single crystals as shown in Fig. 3 gives a superconducting transition temperature  $T_c$  of 88 K for  $x = 0.11$  and 71 K for  $x = 0.28$ . Since a  $T_c$  of 86 K was observed for  $x = 0$  and 84 K for  $x = 0.17$ , the optimum-doped composition is near  $x = 0.1$ . Single crystals with  $x = 0.17$  and 0.28 are in the underdoped region and  $x = 0$  is already in the overdoped region. A metal-insulator transition occurred around  $x = 0.6$ , and  $\text{Bi}_2\text{Sr}_2\text{PrCu}_2\text{O}_{8+\delta}$  ( $x = 1$ ) is an insulator without long-range Pr ordering down to 0.5 K.<sup>16</sup> The diamagnetic response signal decreases systematically with increasing Pr concentration due to the damaging effect on the coherence of the two  $\text{CuO}_2$  layers by the randomly distributed Pr ions between these two layers. Smaller field-cooled (FC) signal as compared with the zero-field-cooled (ZFC) signal indicated the flux trapping by single-crystal defects during the field-cooled process.

The *ab*-plane magnetization curves  $M_{ab}(H, T)$  for four single crystals were measured with  $T < T_c$ . Figure 4 shows  $M_{ab}(H, 5 \text{ K})$  for four samples at 5 K. The *ab*-plane lower critical field  $H_{c1}^{ab}$ , defined as the field at which flux first penetrates, can be estimated from the  $M(H)$  curves as a deviation from the linear  $M$ - $H$  behavior corresponding to the Meissner state. For  $H < H_{c1}$ , the magnetization is reversible and no hysteresis loop was observed. For  $H > H_{c1}$ , the fact that the observed hysteresis loops for these single crystals are near symmetrical denies the effect of surface barriers on the determination of  $H_{c1}$ .<sup>17,18</sup> The *ab*-plane  $H_{c1}^{ab}$  (5 K) thus estimated are 255 G for  $x = 0$ , 170 G for  $x = 0.11$ , 130 G for  $x = 0.17$ , and 95 G for  $x = 0.28$ . For  $x = 0.11$ , increasing temperature gives a lower  $H_{c1}^{ab}$  of 74 G at 10 K, 42 G at 15 K, 22 G at 20 K, and 12 G at 30 K (Fig. 5). Due to the low  $H_{c1}^{ab}$  values, a zero-field de-Gaussing procedure is thoroughly applied before every measurement to ensure the data quality.

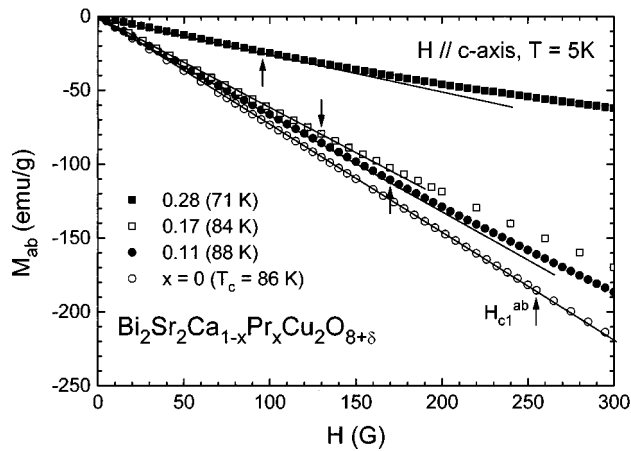


FIG. 4. Magnetization curves  $M_{ab}(H)$  for  $\text{Bi}_2\text{Sr}_2\text{Ca}_{1-x}\text{Pr}_x\text{Cu}_2\text{O}_{8+\delta}$  single crystals ( $x=0, 0.11, 0.17, 0.28$ ) at 5 K. The lower critical field is denoted as  $H_{c1}^{ab}$ .

The  $ab$ -plane lower critical field  $H_{c1}^{ab}$  allow one to estimate the  $ab$ -plane penetration depth  $\lambda_{ab}$  using the equation  $H_{c1} = \Phi_0 \ln \kappa / 4\pi \lambda^2$ , where  $\Phi_0$  is the fluxoid and  $\kappa$  is the Ginzburg-Landau parameter. Using  $\kappa$  of 130 from the parent compound  $\text{Bi}_2\text{Sr}_2\text{CaCu}_2\text{O}_{8+\delta}$  (Ref. 11) for all compounds, the estimated  $\lambda_{ab}$  (5 K) is 1800 Å for  $x=0$ , 2200 Å for  $x=0.11$ , 2500 Å for  $x=0.17$ , and 2900 Å for  $x=0.28$ . The extrapolated  $\lambda_{ab}$  (0 K) of 1650 Å for the parent compound  $\text{Bi}_2\text{Sr}_2\text{CaCu}_2\text{O}_{8+\delta}$  is very close to the value reported using other measurement techniques.<sup>3</sup>

The temperature dependences of the penetration depth  $\lambda_{ab}(T)$  for four single crystals with a magnetic field perpendicular to the  $\text{CuO}_2$  layers are shown collectively in Fig. 6. At lower temperature [ $T < (0.2-0.3)T_c$ ], all samples show a  $T^2$  behavior. However, a crossover from a  $T^2$  to  $T$  dependence was observed at the crossover temperature  $T^* \sim (0.2-0.3)T_c$ . When the temperature is approaching  $T_c$ ,  $\lambda_{ab}$  diverges as expected. The linear  $T$  region is extremely long from  $T^*$  of 16.5 to 55 K for the undoped parent compound  $\text{Bi}_2\text{Sr}_2\text{CaCu}_2\text{O}_{8+\delta}$ , and this linear region shrinks sharply with Pr doping as shown in Fig. 6.

For the clean  $d$ -wave superconductors with line nodes on

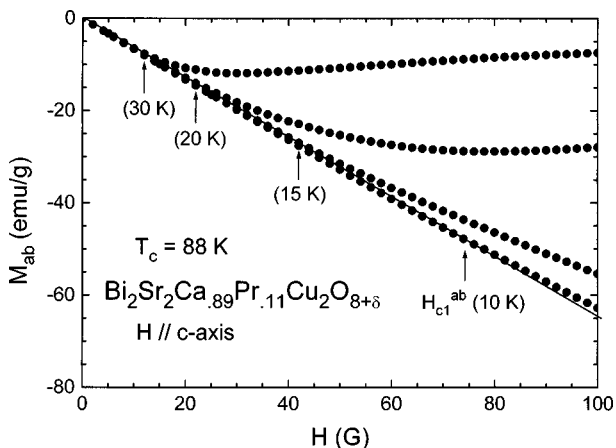


FIG. 5. Magnetization curves  $M_{ab}(H)$  for a  $\text{Bi}_2\text{Sr}_2\text{Ca}_{0.89}\text{Pr}_{0.11}\text{Cu}_2\text{O}_{8+\delta}$  single crystal at 10, 15, 20, and 30 K.

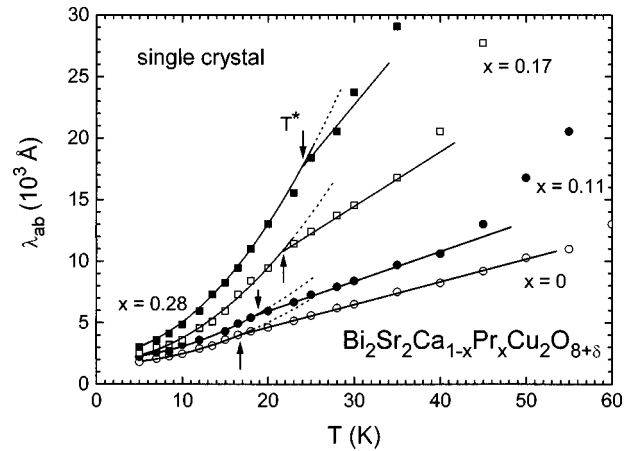


FIG. 6. Temperature dependence of the penetration depth  $\lambda_{ab}$  for  $\text{Bi}_2\text{Sr}_2\text{Ca}_{1-x}\text{Pr}_x\text{Cu}_2\text{O}_{8+\delta}$  single crystals ( $x=0, 0.11, 0.17, 0.28$ ). The crossover temperature from a  $T^2$  behavior to  $T$  dependence is denoted by  $T^*$ .

the Fermi surface, theory predicts a linear  $T$  dependence penetration depth  $\lambda \propto T^p$  ( $p=1$ ) at all temperatures.<sup>10</sup> However, in the present study using impurity-free clean single crystals, the presence of structural modulation and defects for the  $\text{Bi-2212}$ -type phase and the Pr random disordering effect in the Ca site, the defect and disorder scattering will force the clean-limit picture with linear  $T$  dependence to be observed only at higher temperature range, and a crossover to a scattering dominated  $T^2$  dependence ( $p=2$ ) is expected at lower temperature.<sup>10</sup> Such a behavior was observed in the present studies. As shown in Fig. 7, regardless of the  $T_c$  variation from the overdoped to underdoped region,  $T^*$  monotonically increases from 16.5 K for  $x=0$  to 18.9 K for  $x=0.11$ , 21.6 K for  $x=0.17$ , and 24.0 K for  $x=0.28$ . The  $T^*$  values of  $(0.19-0.33)T_c$  are consistent with the theoretical predicted range of  $(0.12-0.27)T_c$ .<sup>10</sup> The reduction of linear  $T$  region and the variation of  $T^*$  with increasing Pr content indicates that Pr acts as a strong scattering center in the Pr-doped  $\text{Bi}_2\text{Sr}_2\text{Ca}_{1-x}\text{Pr}_x\text{Cu}_2\text{O}_{8+\delta}$  system, which modifies the local density of states in the system and is consistent with the prediction for disorder-affected  $d$ -wave superconductors.

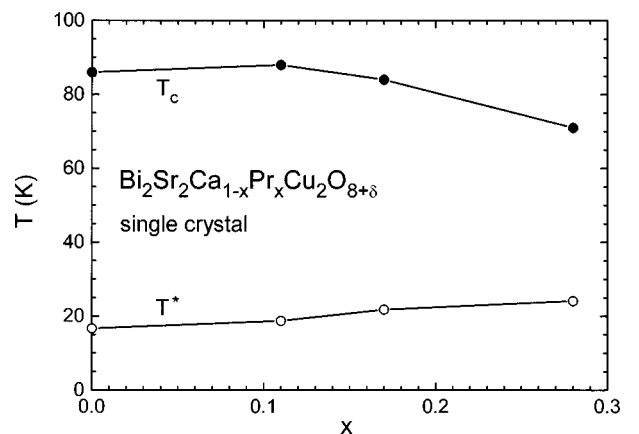


FIG. 7. Variation of the superconducting transition temperature  $T_c$  and crossover temperature  $T^*$  for the  $\text{Bi}_2\text{Sr}_2\text{Ca}_{1-x}\text{Pr}_x\text{Cu}_2\text{O}_{8+\delta}$  system.

## IV. CONCLUSIONS

In conclusion, using impurity-free clean single crystals, the Pr disorder in the  $\text{Bi}_2\text{Sr}_2\text{Ca}_{1-x}\text{Pr}_x\text{Cr}_2\text{O}_{8+\delta}$  system acts as the scattering center and increases the crossover temperature  $T^*$  from a quadratic to linear temperature dependence of the penetration depth  $\lambda_{ab}$ , which is consistent with the theoret-

ically predicted behavior in defect and disorder-affected  $d$ -wave superconductors.

## ACKNOWLEDGMENTS

This work was supported by the Natural Science Foundation and the National Science Council under Contract Nos. NSC87-2112-M007-007 and NSC87-2112-M007-025.

- 
- <sup>1</sup>G. Y. Lee, K. M. Paget, T. R. Lemberger, S. R. Foltyn, and X. D. Wu, Phys. Rev. B **50**, 3337 (1994).
- <sup>2</sup>J. Mao, D. H. Wu, J. L. Peng, R. L. Greene, and S. M. Anlage, Phys. Rev. B **51**, 3315 (1995).
- <sup>3</sup>D. A. Bonn and W. N. Hardy, in *Physical Properties of High Temperature Superconductivity V*, edited by D. M. Ginsberg (World Scientific, Singapore, 1996), p. 7.
- <sup>4</sup>Z. X. Ma, R. C. Taber, L. W. Lombardo, A. Kapitulnik, M. R. Beasley, P. Merchant, C. B. Eom, S. Y. Hou, and J. M. Phillips, Phys. Rev. Lett. **71**, 781 (1993).
- <sup>5</sup>F. Arberg and J. P. Carbotte, Phys. Rev. B **50**, 3250 (1994).
- <sup>6</sup>J. P. Carbotte and C. Jiang, Phys. Rev. B **48**, 4231 (1993).
- <sup>7</sup>M. I. Salkola, A. V. Balatsky, and D. J. Scalapino, Phys. Rev. Lett. **77**, 1841 (1996).
- <sup>8</sup>D. Achkir, M. Poirier, D. A. Bonn, R. Liang, and W. N. Hardy, Phys. Rev. B **48**, 13 184 (1993).
- <sup>9</sup>A. Maeda, T. Shibauchi, N. Kondo, K. Uchinokura, and M. Kobayashi, Phys. Rev. B **46**, 14 234 (1992).
- <sup>10</sup>P. J. Hirschfeld and N. Goldenfeld, Phys. Rev. B **48**, 4219 (1993).
- <sup>11</sup>O. Waldmann, F. Steinmeyer, P. Muller, J. J. Neumeier, F. X. Regi, H. Savary, and J. Schneck, Phys. Rev. B **53**, 11 825 (1996).
- <sup>12</sup>Y. Gao, P. Pernambuco-Wise, J. E. Crow, J. O'Reilly, N. Spencer, H. Chen, and R. E. Salomon, Phys. Rev. B **45**, 7436 (1992).
- <sup>13</sup>V. P. S. Awana, S. K. Agarwal, A. V. Narlikar, and M. P. Das, Phys. Rev. B **48**, 1211 (1993).
- <sup>14</sup>V. P. S. Awana, L. Menon, and S. K. Malik, Phys. Rev. B **51**, 9379 (1995); **53**, 2245 (1996).
- <sup>15</sup>X.-G. Li (unpublished).
- <sup>16</sup>H. C. Ku, T. I. Hsu, Y. Y. Hsu, T. J. Lee, K. W. Yeh, Y. Huang, J. Y. Lin, S. J. Chen, H. D. Yang, Y. Y. Chen, J. C. Ho, and X.-G. Li, Chin. J. Phys. **35**, 903 (1997).
- <sup>17</sup>L. Burlachkov, Phys. Rev. B **47**, 8056 (1993).
- <sup>18</sup>L. Fabrega, J. Fontcuberta, B. Martinez, and S. Pinol, Phys. Rev. B **50**, 3256 (1994).